12

Polarization Detection of Molecular Alignment Using Femtosecond Laser Pulse

Nan Xu, Jianwei Li, Jian Li, Zhixin Zhang and Qiming Fan
National Institute of Metrology
China

1. Introduction

Femtosecond laser is becoming a powerful tool to manipulate the behaviors of molecules. When molecules are irradiated by strong laser field with intensity below the ionization threshold of molecules, the interaction between molecules and the laser electric field tends to align the molecules with the most polarizable axis along the laser polarization vector. If the laser pulse duration is larger than the rotational period of the molecule, the free rotor transforms into a pendular state that liberates about the polarization vector. Upon turning off the laser, the librator adiabatically returns to the isotropic free rotator from which it originates. If the laser pulse duration is less than the molecular rotational period, the laser-molecule interaction gives the molecules a rapid "kick" to make the molecular axis toward the laser field vector. After extinction of the laser, the transient alignment can periodically revive as long as the coherence of the rotational wave packet is preserved. Therefore, the former is also called adiabatic alignment and the latter field-free alignment. Even though both adiabatic alignment and field-free alignment can produce macroscopic ensembles of highly aligned molecules, field-free alignment has the obvious advantages that will not interfere with subsequent measurements. A variety of new and exciting applications of field-free aligned molecules are currently emerging. For example, Litvinyuk *et al.* measured strong field laser ionization of aligned molecules and obtained directly the angle dependent ionization rate of molecules by intense femtosecond laser field. Another novel application is to accomplish a tomographic reconstruction of the highest occupied molecular orbital of nitrogen by using high harmonic generation from intense femtosecond laser pulses and aligned molecules. Recently, Kanai *et al.* observed the quantum interference during high-order harmonic generation from aligned molecules and demonstrated that aligned molecules could be served as an ideal quantum system to investigate the quantum phenomena associated with molecular symmetries. The weak field polarization technique has homodyne and heterodyne detection modes. The alignment signal is proportional to $(\langle\cos^2\theta\rangle - 1/3)^2$ for homodyne detection and $(\langle\cos^2\theta\rangle - 1/3+C)^2$ for heterodyne detection, where C describes the constant external birefringence contribution. Because the magnitude and the polarity of the external birefringence are hard to precisely control, homodyne detection is commonly used up to now. However, the homodyne signal cannot indicate whether the $\langle\cos^2\theta\rangle$ is larger or smaller than 1/3. In other words, the homodyne signal cannot demonstrate whether the aligned molecule is parallel or perpendicular to the laser

polarization direction. Using the heterodyne method, the alignment signals directly reproduce the alignment parameter<cos² θ>.

1.1 Angle-dependent AC stark shift

Any non-spherical polarizable particle placed in an electric field will experience a torque due to the angular-dependent interaction (potential) energy U between the induced dipole moment $\vec{p} = \vec{\alpha} \cdot \vec{\varepsilon}$ and the field $\vec{\varepsilon}$. Consider, for simplicity, a linear particle having one dominant axis of polarizability $\alpha_{\|} > \alpha_{\perp}$ as shown in Figure 1. When placed in the field $\vec{\varepsilon}$ the potential energy is given by $U = -\vec{p} \cdot \vec{\varepsilon}$. The change in the potential energy for a small change of the field strength d $\vec{\varepsilon}$ would be

$$dU = -\vec{p} \cdot d\vec{\varepsilon} = -p_{//} d\varepsilon_{//} - p_{\perp} d\varepsilon_{\perp} \tag{1}$$

where the directions || and ⊥ are parallel and perpendicular to the dominant axis of the particle. After substitution of the components of the induced dipole moment $p_i = \alpha_i \varepsilon_i$, dU becomes

$$dU = -\alpha_{//} \varepsilon_{//} d\varepsilon_{//} - \alpha_{\perp} \varepsilon_{\perp} d\varepsilon_{\perp} \tag{2}$$

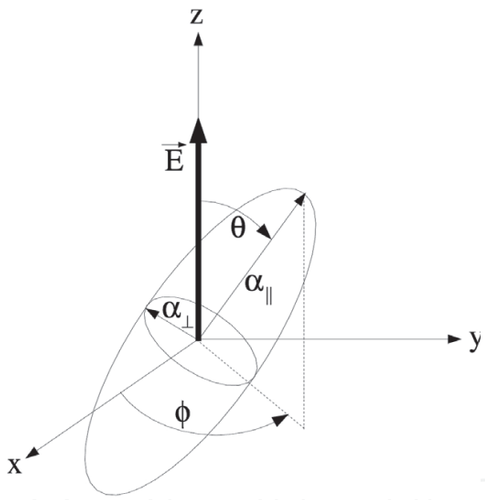

Fig. 1. Geometry of an anisotropic particle in an electric field $\vec{\varepsilon}$.

which can be integrated to give

$$U = -\frac{1}{2}[\alpha_{//}{}^2 \varepsilon_{//}{}^2 + \alpha_{\perp}{}^2 \varepsilon_{\perp}{}^2] \tag{3}$$

By using the angle θ between the dominant axis of the particle and the electric field $\vec{\varepsilon}$ this can be written as

$$\begin{aligned} U(\theta) &= -\frac{1}{2}[\alpha_{//}{}^2 \varepsilon^2 \cos^2\theta + \alpha_{\perp}{}^2 \varepsilon^2 \sin^2\theta] \\ &= -\frac{1}{2}\alpha_{\perp} \varepsilon^2 - \frac{1}{2}\Delta\alpha \varepsilon^2 \cos^2\theta \end{aligned} \tag{4}$$

with $\Delta\alpha=(\alpha_{\parallel} - \alpha_{\perp})$.
This potential contains a constant term and an angular-dependent term. The constant term, however, is just a coordinate-independent shift which does not introduce any torques and can hence be dropped for convenience. Furthermore, when dealing with the particular case of diatomic molecules placed in infrared or near-infrared laser fields $\varepsilon(t) \sim \varepsilon_0 \sin\omega t$ which are far off-resonant with rotational frequencies, as is typical in experiments of strong field control of molecular rotations, the oscillating electric field switches direction too fast for the nuclei to follow directly. These oscillations can be removed from the potential energy by considering instead the time-average of the energy $U(\theta)$ over one cycle

$$\begin{aligned} U(\theta,t) &= \int_0^{2\pi} \frac{1}{2}\Delta\alpha\varepsilon_0{}^2 f^2(t)\sin^2(t')\cos^2\theta dt' \\ &= -\frac{1}{4}\Delta\alpha\varepsilon_0{}^2 f^2(t)\cos^2\theta \end{aligned} \tag{5}$$

where ε_0 is the maximum field strength of the laser and f(t) represents the envelope of the laser pulse which varies much slower than the field oscillations. This laser induced potential energy is known as the angular AC Stark shift. Note that any permanent dipole of the molecule would give a zero contribution to the potential energy upon time-averaging over one cycle of the laser field.

1.2 Quantum evolution

When the laser pulse interacts with the molecular gas, rotational wave packets are created in each molecule. The particular wave packet created in a given molecule will depend on its initial angular momentum state. Hence, to calculate the response of the molecular medium, the induced wave packet starting from each initial state in the thermal distribution must be calculated.
Consider a laser pulse with the electric field linearly polarized along the z-axis as in Figure 1. The interaction of laser pulse with the molecule is described by the Schrödinger equation

$$i\hbar\frac{\partial\psi(t)}{\partial t} = (BJ^2 - U_0(t)\cos^2\theta)\psi(t) \tag{6}$$

where θ is the angle between the laser polarization and the molecular axis, BJ^2 is the rotational energy operator, and

$$U_0(t) = \frac{\Delta\alpha\varepsilon_0^2}{4}\sin^2(\frac{\pi t}{2\tau_{on}}) \tag{7}$$

where τ_{on} gives the time for the pulse to rise from zero to peak amplitude and is also the full width at half maximum (FWHM) of the $\sin^2$ pulse.
The evolution of the wave function for the duration of the aligning pulse was calculated numerically in the angular momentum basis |J, M> .The time-dependent wave function is first expanded in the |J, M> basis

$$\psi(t) = \sum_{J,M} A_{J,M}(t)\left|J,M\right\rangle \tag{8}$$

Where |J, M> is the spherical harmonics function, and $A_{J,M}$ (t) is the expansion coefficient.
In this basis, the Hamiltonian H(t) = [BJ^2 -U_0(t) $\cos^2\theta$] becomes

$$\begin{aligned}&\langle J,M|H(t)|\Psi(t)\rangle\\&=B_0J(J+1)A_{J,M}-U_0(t)C_{J,J+2,M}A_{J+2,M}-U_0(t)C_{J,J,M}A_{J,M}-\\&U_0(t)C_{J,J-2,M}A_{J-2,M}\end{aligned}\tag{9}$$

Where

$$\begin{aligned}C_{J,J,M}&=\langle J,M|\cos^2\theta|J,M\rangle\\C_{J,J+2,M}&=\langle J,M|\cos^2\theta|J+2,M\rangle\\C_{J,J-2,M}&=\langle J,M|\cos^2\theta|J-2,M\rangle\end{aligned}\tag{10}$$

The Hamiltonian (9) does not couple even and odd J. All transitions occur between J ~J + 2 and J ~ J-2. This is a consequence of the symmetry of the angular potential $\cos^2\theta$ with respect to the point $\theta=\pi/2$. Furthermore, different M states do not couple. This is a consequence of the cylindrical symmetry of the angular potential.
With the rotational superposition at the end of the pulse expanded in angular momentum states

$$\psi(t)=\sum_{J,M}A_{J,M}|J,M\rangle\tag{11}$$

the field-free evolution of the wave packet becomes

$$\psi(t)=\sum_{J,M}A_{J,M}e^{-i(E_J/\hbar)t}|J,M\rangle\tag{12}$$

where E_J is the eigenenergy，$E_J=BhcJ(J+1)$.
Using these energies, the field-free evolution given by Equation (12) is

$$\psi(t)=\sum_{J,M}A_{J,M}e^{-iBhcJ(J+1)t/\hbar}|J,M\rangle\tag{13}$$

Setting $t=\pi/B_0$ gives

$$\begin{aligned}\psi(t=1/2Bc)&=\sum_J A_J e^{-iBhcJ(J+1)(1/2Bc)/\hbar}|J,M\rangle\\&=\sum_J A_J e^{-iJ(J+1)\pi}|J,M\rangle\\&=\sum_J A_J|J,M\rangle=\psi(t=0)\end{aligned}\tag{14}$$

where the fact that J(J+1) is always an even integer and hence exp[-iJ(J+1)π] =1 was used. This shows that after a field-free evolution of $t=\pi/B_0$ the wave function will exactly reproduce the wave function at t = 0. Such behavior is called a wave-packet revival.

1.3 Measurement of alignment

The standard measure of alignment is defined in a slightly different way and is given by the average value of $\cos^2\theta$, where θ is the angle between the laser polarization direction and the molecular axis.

$$<\cos^2\theta>=\langle\Psi|\cos^2\theta|\Psi\rangle \tag{15}$$

This measure would give a value of $<\cos^2\theta>=1$ for an angular distribution perfectly peaked along the 'poles' $\theta=0$ andπ, $<\cos^2\theta>=0$ for a distribution peak along the 'equator' $\theta=\pi/2$, and $<\cos^2\theta>=1/3$ for an isotropic distribution evenly distributed across all θ. If $<\cos^2\theta>>1/3$, the molecule is predominantly aligned along the laser polarization direction. If $<\cos^2\theta><1/3$, the probability distribution for the axis of the molecule is concentrated around a plane orthogonal to the laser polarization direction and labeled as an antialignment molecule.

During the interaction with the laser pulse, this measure is simply obtained by numerical integration over the computed wave function. For field-free propagation, the time-dependent measure of alignment is given by

$$\begin{aligned}&<\cos^2\theta>(t)_{J_0,M_0}=\langle\Psi|\cos^2\theta|\Psi\rangle\\&=\sum_J|A_{J,M}|^2C_{J,J,M}+|A_{J,M}||A_{J+2,M}|C_{J,J+2,M}\cos(\omega_J t+\varphi)\end{aligned} \tag{16}$$

where $\omega_J=(E_{J+2}-E_J)$.ϕ denotes the relative phase between the states |J, M> and |J+2, M> at the start of the field-free evolution. Note that during the field-free evolution the $<\cos^2\theta>$ (t) signal is composed of the discrete frequencies ω_J.

The alignment signal is further averaged over an initial Boltzmann distribution of angular momentum states for a given initial temperature T. This is accomplished by calculating the rotational wave-packet dynamics for each initial rotational state in the Boltzmann distribution, and then incoherently averaging the $<\cos^2\theta>(t)_{J,M}$ signal from each initial state |J, M> weighted by the Boltzmann probability

$$<\cos^2\theta>(t)=\frac{\sum_{J_0,M_0}\exp(-E_{J_0}/kT)<\cos^2\theta>(t)_{J_0,M_0}}{\sum_{J_0}(2J_0+1)\exp(-E_{J_0}/kT)} \tag{17}$$

2. Measurement of molecular alignment

Now, the experimentalists have developed two typical methods to evaluate experimentally the alignment degree of molecules. The first one is realized by breaking the aligned molecule through multielectron dissociative ionization or dissociation followed by ionization of the fragments. The alignment degree $<\cos^2\theta>$ was thus deduced from the angular distribution of the ionized fragments. The disadvantage for this method is that the probe laser is so strong that destroys the aligned molecules. The second one is the weak field polarization spectroscopy technique based on the birefringence caused by aligned molecules. The advantage for this method is that the probe laser is so weak that it neither affects the alignment degree nor destroys the aligned molecules.

The first section outlines the homodyne detection method to measure alignment of different gas molecules. The enhanced field-free alignment is also demonstrated here. The second section outlines the heterodyne detection method and the numerical calculation of molecular alignment. In this section, field-free alignment signals and the population of rotational states of diatomic molecules are present. The last section is the detection of gas component using molecular alignment, in which a feasibility of rapid detection of gas component is shown.

2.1 Measurement of molecular alignment

We report our results about field-free alignment of diatomic molecules (N_2, O_2, CO) and polyatomic molecules (CO_2, CS_2, C_2H_4) at room temperature under the same laser properties. We also demonstrated experimentally that the alignment degree could be strongly enhanced by using double pulses at a separated time delay. These researches provide a feasible approach to prepare field-free highly aligned molecules in the laboratory for practical applications.

2.1.1 Experimental setup

Figure2 shows the experimental setup of the molecular alignment measurement. The laser system consists of a chirped pulse amplified Ti:sapphire system operating at 800nm and a repetition rate of 10Hz. The laser pulse of 110fs was split into two parts to provide a strong energy pump beam and a weak energy probe beam both linearly polarized at 45° with respect to each other. For double pulses alignment of molecules, the strong pump laser was split into another two aligning pulses with equal intensity. The relative separated times between the two pulses is precisely adjusted using an optical translational stage controlled by a stepping motor. Both the pump beam and the probe beam are focused with a 30cm focal length lens into a 20cm long gas cell at a small angle. The gas cell was filled with different gases at room temperature under one atmosphere pressure. The field-free aligned molecules induced by the short pump laser will cause birefringence and depolarize the probe laser. After the cell, the depolarization of the probe, which represents the alignment degree, is analyzed with a polarizer set at 90°with respect to its initial polarization detection. In order to eliminate the laser fluctuation, a reference laser was introduced. The alignment signals and the reference laser signals were detected by two homotypical photoelectric cells and transformed into a computer via a four-channel A/D converter for analysis.

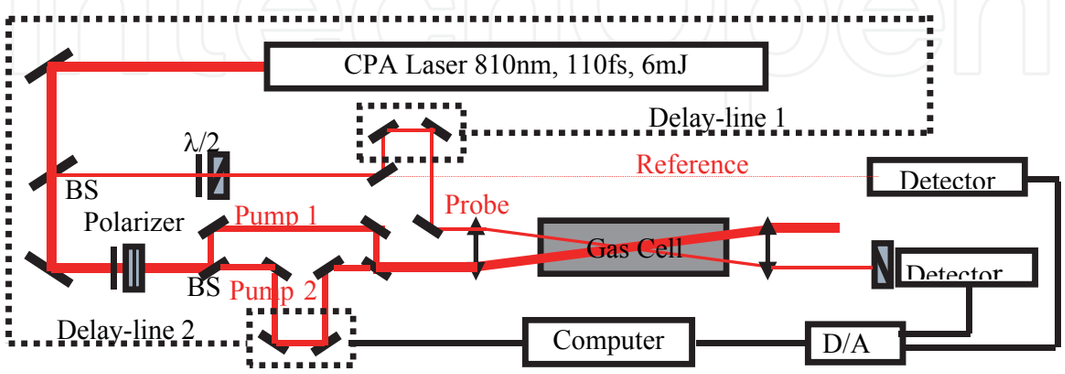

Fig. 2. Experimental setup for measuring field-free alignment of molecules induced by femtosecond laser pulse. BS: beam splitter.

2.1.2 Results and discussion

Figure 3 shows the alignment signal for diatomic molecules (a) N_2, (b) O_2, and (c) CO irradiated by 800nm, 110fs at an intensity of 6×10^{13} W/cm^2. The classical rotational period T_r of molecules is determined by the equation $T_r = 1/2\ B_0\, c$ where B_0 is rotational constant in the ground vibronic state and c is the speed of the light. For N_2, O_2 and CO, B_0 is 2.010, 1.4456, 1.9772 cm^{-1}, respectively. The corresponding rotational period T_r is therefore 8.3 ps for N_2, 11.6 ps for O_2 and 8.5 ps for CO. It is clearly noted from figure 3 that the alignment signal fully revives every molecular rotational period. However, there are also moments of strong alignment that occur at smaller intervals. The difference at quarter full revival for N_2, O_2 and CO can be well explained by the different nuclear spin weights of the even and odd J states in the initial distribution. At 1/4, 3/4, 5/4, … full revivals, the odd wave packet has maxima (minima) whereas the even wave packet has minima (maxima). For homonuclear diatomic molecules, the nuclear spin statistics controls the relative weights between even and odd J states. In the case of N_2, the relative weights of the even and odd J are 2:1. As a result, the temporary localization of the even wave packet at T_r /4 is only partially cancelled by its odd counterpart. Thus, some net N_2 alignment and antialignment is observed near t = $n\ T_r$ /4, where n is an odd number. In the case of O_2, only odd J states are populated. Since only a single localized wave packet exists, strong net alignment and antialignment is observed near the time of a quarter revivals. For heteronuclear diatomic molecule CO, the even and odd J states are equally populated, the opposite localizations would cancel and therefore no net alignment would be observed at the time of the quarter revival.

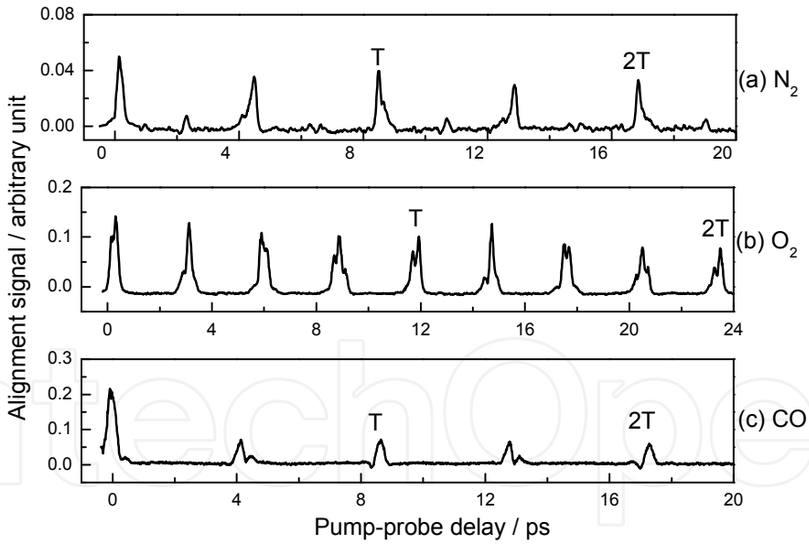

Fig. 3. Field-free alignment signal for diatomic molecules (a) N_2, (b) O_2, and (c) CO irradiated by 800nm, 110fs at an intensity of 6×10^{13} W/cm^2.

Figure 4 shows the alignment signal for polyatomic molecules (a) CO_2, (b) CS_2, and (c) C_2H_4 irradiated by 800nm, 110fs at an intensity of 6×10^{13} W/cm^2. The classical rotational period T_r is 42.7 ps for CO_2, 152.6 ps for CS_2 and 9.3 ps for C_2H_4. It can clearly be seen that the alignment signal repeats every molecular rotational period. Note that although CO_2 is not actually a homonuclear diatomic, the two O atoms are indistinguishable. Hence symmetrization of the wave function with respect to these two particles require that only

even *J* states are populated. Since only a single localized wave packet exists, strong net alignment and antialignment is observed near the time of a quarter revivals. For the same reason, the net alignment and antialignment is also observed near the time of a quarter revival for CS_2. In a recent theoretical paper, Torres *et al.* explicitly calculated the angular distribution of CS_2 ensemble as they evolve through a rotational revival. They found the ensemble deploys a rich variety of butterfly-shaped distribution, presenting always some degree of order between the aligned and antialigned distributions. Unlike the linear molecules, complicated revival signals were observed for C_2H_4 because of its asymmetric planar structure. Our experimental observation of C_2H_4 well agreed with theoretical calculation carried out by Underwood *et al*. Those authors also proposed a theoretical scheme to realize three-dimensional field-free alignment of C_2H_4 by using two orthogonally polarized, time-separated laser pulses.

In Figure 4, it can also be seen that the alignment signal does not return to background signal with probe laser preceding the aligned laser, especially for CS_2. The increased background signal results from the permanent alignment of the molecules, in which the laser-molecule interaction spreads each initial angular momentum state to higher *J* but does not change *M*. Thus, rather than being uniformly distributed, the angular momentum vectors of each *J* state in the wavepacket are preferentially oriented perpendicular to the aligning pulse polarization. Due to the relaxation of the rotational population, the permanent alignment will decay monotonically under field-free conditions towards its thermal equilibrium.

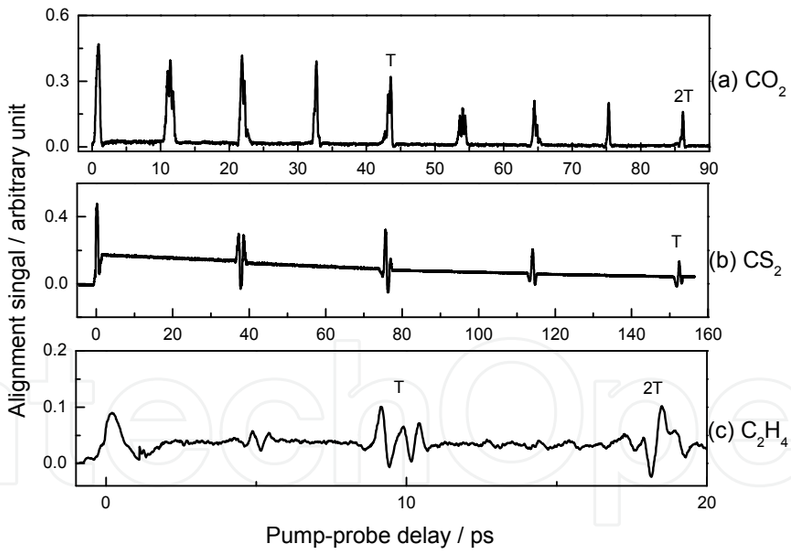

Fig. 4. Field-free alignment signal for diatomic molecules (a) CO_2, (b) CS_2, and (c) C_2H_4 irradiated by 800nm, 110fs at an intensity of 6×10^{13} W/cm^2.

For real applications, it is important to ensure the higher degree of alignment obtained under field-free condition. Theoretical investigation indicated that the degree of alignment could be improved by minimizing the rotational temperature of the molecules or by increasing the laser intensity. For practical application, minimizing the rotational temperature is not a good approach. Therefore, we studied the field-free alignment of molecules by varying laser intensity.

However, the maximum degree of alignment thus obtained is limited by ionization of the molecule in the laser. In order to obtain highly aligned molecules without destroying the molecule, theorists proposed multiple pulse method, in which alignment is created with a first pulse, and then the distribution is squeezed to a higher degree of alignment with subsequent pulses. Thus multiple-pulse method gets around the maximum intensity limit for single laser pulse and highly aligned molecules can be obtained without destroying the molecule.

The enhanced field-free alignment of CS_2 by means of two-pulse laser was also experimentally performed, in which the aligning laser was divided into two beams with equal intensity of 2×10^{13} W/cm^2. Figure 5 clearly shows the timing for the two aligning laser pulses and the probe laser pulse. The first aligning laser pulse prepares a rotational wave packet at time zero and the second aligning laser pulse modifies this rotational wave packet at $T_r/4$. The probe laser pulse measures the alignment degree of molecules at $3T_r/4$. Thus the probe laser measured the alignment signal at $3T_r/4$ when the first aligning laser worked alone, which is shown in red line in the inset of Figure 5. The probe laser measured the alignment signal at $T_r/2$ when the second aligning laser worked alone, which is shown in blue line in the inset of Figure 5. Depending on the delay time between the first aligning and the second aligning laser pulses, the field-free alignment can be instructive or destructive. With a proper adjustment of the delay between the two aligning laser pulses, an obvious enhanced alignment signal is observed in the probe region, as well as the permanent alignment, which is shown in black line in the inset in Figure 5. The optimal delay of the second aligning laser pulses is typically located before the maximum alignment during a strong revival after the first aligning laser pulse. With such a timing, the second aligning laser pulse catches the molecules as they are approaching the alignment peak and pushes them a bit more toward an even stronger degree of alignment. The region of increased alignment will appear in subsequent full revivals from this point. Therefore, it is very promising that field-free highly aligned molecules can be obtained using multiple pulses.

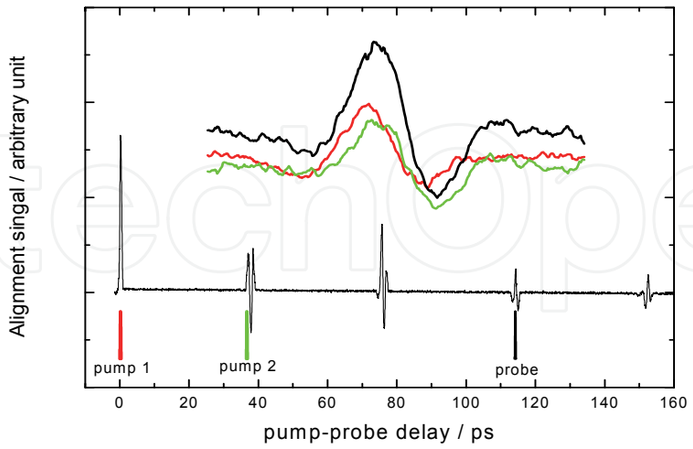

Fig. 5. (Lower) Single-pulse alignment signal illustrates pulse timing for double-pulse experiment. (Upper) Red line represents the alignment signal at $3T_r/4$ induced by the first aligning laser pulse alone, blue line represents the alignment signal at $T_r/2$ induced by the second aligning laser pulse alone, black line represents the enhanced alignment signal induced by the two aligning laser pulses with appropriate separated times.

2.2 Heterodyne detection of molecular alignment

The weak field polarization technique has homodyne and heterodyne detection modes. The alignment signal is proportional to ($<\cos^2\theta>-1/3$) ^{2} for homodyne detection and ($<\cos^2\theta>-1/3$) for pure heterodyne detection. Comparing with the homodyne signal, pure heterodyne signal had the merit of directly reproducing the alignment parameter $<\cos^2\theta>$ except a 1/3 baseline shift. Unfortunately, the pure heterodyne signal is hardly obtained in the experimental measurement; homodyne detection is still commonly used till now. However, the homodyne signal does not indicate whether the aligned molecule is parallel or perpendicular to the laser polarization direction.

We modified the typical weak field polarization technique. Both homodyne and pure heterodyne detection were realized in this experimental apparatus. They were employed to quantify the post-pulse alignment of the diatomic molecules irradiated by a strong femtosecond laser pulse. The alignment signal and its Fourier transform spectrum were analyzed and compared with the numerical calculation of the time-dependent Schrödinger equation.

2.2.1 Theory

The state vector of the free molecule denoted by Φ(t) was probed by a non-resonant weak laser pulse

$$\overrightarrow{\varepsilon_d} = \vec{e}E_{probe}\exp(-i\omega(t-\tau)) \tag{18}$$

where E_{probe} denotes the electric field envelope of the incident probe laser and τ is the time delay between the pump and the probe laser pulses. After traveling in the aligned molecules, the linearly polarized probe laser depolarized and became elliptical. The ellipticity was determined by the average of the field-induced dipole moment under the state vector Φ(t). Using a polarizer orthogonal to the probe field, the depolarization of the probe laser was measured. With the approximation of slowly varying envelope and small amplitude, the signal field was described by the wave equations [18]. After the integral over the state vector Φ(t), the signal field was:

$$E_s(\tau) = \frac{3\,l\Delta\alpha N\omega}{8c}(<\cos^2\theta>_\tau - \frac{1}{3})E_{probe}\exp(i\pi/2) \tag{19}$$

where l is the distance that the probe laser traveled in the aligned molecules, ω is the laser frequency, $\Delta\alpha=(\alpha_{\parallel}-\alpha_{\perp})$is the anisotropy of the molecular dynamical polarizability, N is the molecular number density, C is the speed of the light. It should be mentioned that there was a π/2 phase shift between the signal field $E_S(\tau)$ and the probe laser electric field E_{probe}. The aforementioned alignment signal is commonly measured homodyne signal. The field-induced birefringence is accessed by measuring the ellipticity of an initially linearly polarized laser field traveling through the aligned molecules.

When the probe laser polarization was a little off from the optic axis of the quarter wave plate (δ ~ 5°), the linearly polarized probe laser became elliptical after the quarter wave plate.

$$\vec{E}_{probe}(\tau) = \vec{e}_X E_X\exp[-i\omega(t-\tau)] + \vec{e}_Y E_Y\exp[-i\omega(t-\tau)\pm i\pi/2] \tag{20}$$

There is a π/2 phase shift between E_X and E_Y. The sign of the phase shift is determined by the polarization direction of the linearly polarized laser relative to the main optical axis of the quarter wave plate. In addition to $E_S(\tau)$, a constant external electric field E_Y is also collected by the detector. The detection becomes heterodyne. The signal intensity is determined by:

$$\begin{aligned} I_{sig}(\tau) &= \eta \int_{\tau - T_d/2}^{\tau + T_d/2} \left| E_s(\tau) + E_Y \exp[-i\omega(t-\tau) \pm i\pi/2] \right|^2 dt \\ &= \eta \int_{\tau - T_d/2}^{\tau + T_d/2} \left| \frac{3\, l\, \omega\, \Delta\alpha\, N}{8c} (< \cos^2\theta >_\tau - \frac{1}{3}) E_X \exp(-i\omega(t-\tau) + i\frac{\pi}{2}) + E_Y \exp[-i\omega(t-\tau) \pm i\frac{\pi}{2}] \right|^2 dt \\ &\propto [(< \cos^2\theta >_\tau - \frac{1}{3}) + C]^2 \end{aligned} \quad (21)$$

where T_d is the response time of the detector and much longer than the pulse width of the probe laser, η is the detection efficiency. The magnitude of the parameter

$$C = \frac{8\, c\, tg\delta}{3\, l\, \omega\, \Delta\alpha\, N}, \quad (22)$$

which denotes the contribution of the external electric field, is determined by the ellipticity

$$\varepsilon = \frac{E_Y}{E_X} = |tg\delta| \quad (23)$$

The sign of the parameter C, which denotes the polarity of the external electric field, is determined by the rotation direction of the elliptical polarized probe laser after the quarter wave plate.

The pure heterodyne signals are derived from the difference between the two heterodyne signals under the existence of an external electric field with opposite polarity and equal magnitude.

$$\begin{aligned} & I_{sig}^{positive}(\tau) - I_{sig}^{negative}(\tau) \\ & \propto \left\{ [(< \cos^2\theta >_\tau - \frac{1}{3}) + |C|]^2 - [(< \cos^2\theta >_\tau - \frac{1}{3}) - |C|]^2 \right\} \\ & = 4|C|(< \cos^2\theta >_\tau - \frac{1}{3}) \end{aligned} \quad (24)$$

The above equation clearly demonstrates that the alignment signal is proportional to (<cos² θ>-1/3) for pure heterodyne detection.

2.2.2 Experimental setup

An 800 nm, 110 fs laser pulse was divided into two parts to provide a strong energy pump beam and a weak energy probe beam, both linearly polarized at 45° with respect to each other. An optical translational stage controlled by a stepping motor was placed on the pump beam path in order to precisely adjust the relative separation times between the two pulses. Both the pump beam and the probe beam were focused with a 30 cm focal length lens into a

20 cm long gas cell at a small angle. The gas cell was filled with different gases at room temperature under one atmospheric pressure. The field-free aligned molecules induced by the strong pump laser caused birefringence and depolarized the probe laser. The depolarization of the probe laser, which represents the alignment degree, was analyzed with a polarizer set at 90° with respect to its initial polarization direction. The alignment signals were detected by a photoelectric cell and transformed into a computer via a four-channel A/D converter for analysis.

The main modification was that a λ/4 wave plate was inserted on the probe laser path before the gas cell. Figure 1 also shows the relative directions of the laser polarizations, the optic axis of the quarter wave plate and the signal field. The optic axis of the quarter wave plate was along X direction, 45° with respect to the pump laser polarization. The signal electric field in Y direction was collected by a detector. When the probe laser polarization was along the optic axis of the quarter wave plate, this was the common used homodyne detection. When the probe laser polarization was a little off from the optic axis of the quarter wave plate (δ ~ 5°), the linearly polarized probe laser became elliptical after the quarter wave plate. In addition to the transient birefringence caused by the aligned molecules, a constant external electric field is also collected by the detector. The detection becomes heterodyne. The pure heterodyne signals are derived from the difference between the two heterodyne signals under the existence of an external electric field with opposite polarity and equal magnitude.

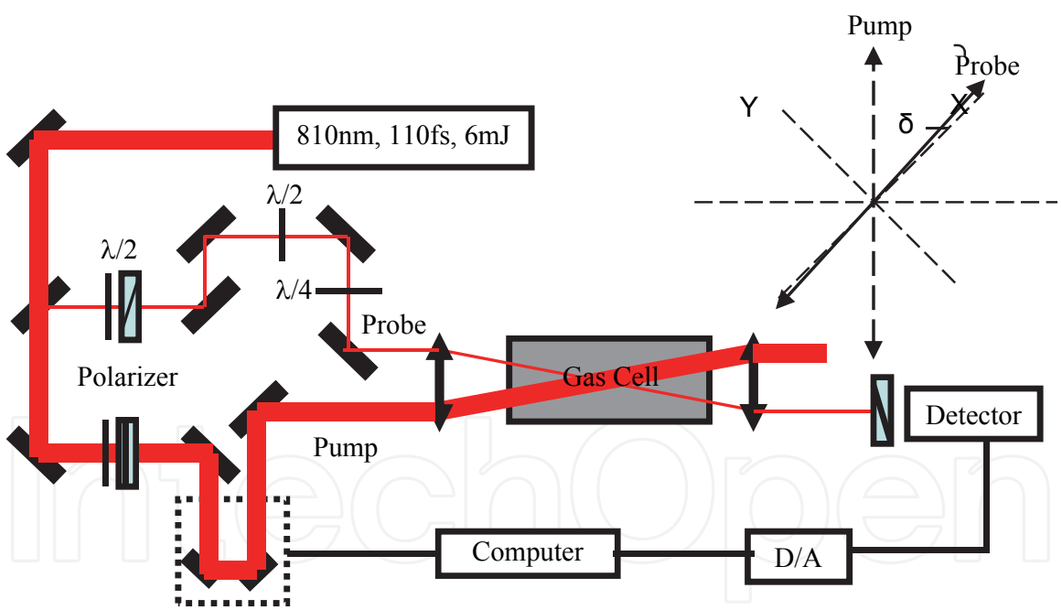

Fig. 6. Experimental setup for measuring field-free alignment of molecules induced by strong femtosecond laser pulses. The optic axis of the quarter wave plate was along X direction, 45° with respect to the pump laser polarization. The signal electric field in Y direction was collected by a detector.

2.2.3 Results and discussion

1. Field-free alignment

The calculated revival structures of N_2, O_2 and CO irradiated by 800 nm, 110 fs laser pulses at an intensity of 2×10^{13} W/cm^2 are shown in Figures 7a, 8a and 9a, respectively. The

baseline value of $\langle\cos^2\theta\rangle$ is about 0.334, approximating an isotropic distribution of 1/3. The classical rotational period Tr of molecules is determined by the equation $Tr = 1/(2B_0 c)$, where B0 is the rotational constant of the diatomic molecule in the vibrational ground state and c is the speed of the light. For N_2, O_2 and CO, B0 is 2.010, 1.4456 and 1.9772 cm^{-1}, respectively. The corresponding rotational period Tr is therefore 8.3 ps for N_2, 11.6 ps for O_2 and 8.5 ps for CO.

The alignment signal fully revives every molecular rotational period. There are also moments of strong alignment that occur at shorter intervals. However, the three molecules exhibit different behaviors at the quarter full revivals. The ratios of the alignment signal at quarter revivals to that at full revivals were nearly 1/3 for N_2, 1 for O_2 and 0 for CO. The large difference at quarter full revivals for N_2, O_2 and CO results from the different nuclear spin weights of the even and odd J states in the initial distribution. At quarter full revivals, the odd wave packet has maxima (minima), whereas the even wave packet has minima (maxima). For homonuclear diatomic molecules, the nuclear spin statistics control the relative weights between even and odd J states. In the case of N_2, the relative weights of the even and odd J are 2:1. As a result, the temporary localization of the even wave packet at quarter full revival was partially cancelled by its odd counterpart. Thus, the alignment signal at the quarter full revival was about 1/3 of that at the full revival for N_2. In the case of O_2, only odd J states were populated. Since only a single localized wave packet existed, the alignment signal at the quarter full revival was almost equal to that at the full revival for O_2. For the heteronuclear diatomic molecule CO, the opposite localizations of the even and the odd wave packets would cancel each other. Therefore, no net alignment would be observed at the time of the quarter full revival.

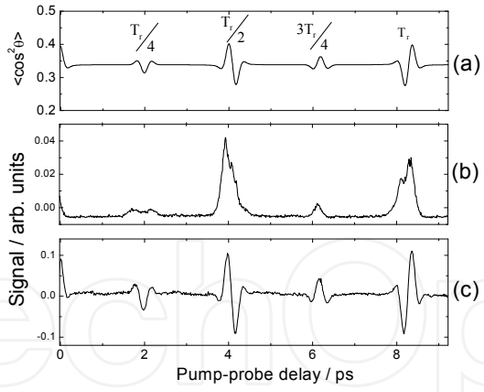

Fig. 7. Revival structure of N_2 irradiated by 800 nm, 110 fs at an intensity of 2×10^{13} W/cm^2 (a) numerical calculation, (b) homodyne signal, (c) pure heterodyne signal.

Figures 7b, 8b and 9b display the homodyne signal versus the pump-probe delay for N_2, O_2 and CO irradiated by 800 nm, 110 fs laser pulses at an intensity of 2×10^{13} W/cm^2. The signal was proportional to $(\langle\cos^2\theta\rangle - 1/3)^2$. Each peak denotes the alignment moment with the molecular axis parallel to the pump laser polarization direction ($\langle\cos^2\theta\rangle > 1/3$) or perpendicular to the pump laser polarization direction ($\langle\cos^2\theta\rangle < 1/3$). For the intervals between the alignments, the angular distribution of the molecules was isotropic relative to the laser polarization direction ($\langle\cos^2\theta\rangle = 1/3$). Although the homodyne signal clearly

determined the moment that the alignment occurred, it could not indicate whether the aligned molecules were parallel or perpendicular to the laser polarization direction.

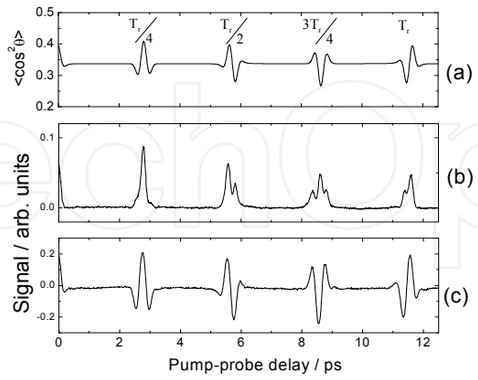

Fig. 8. Revival structure of O_2 irradiated by 800 nm, 110 fs at an intensity of 2×10^{13} W/cm^2 (a) Numerical calculation, (b) homodyne signal, (c) pure heterodyne signal.

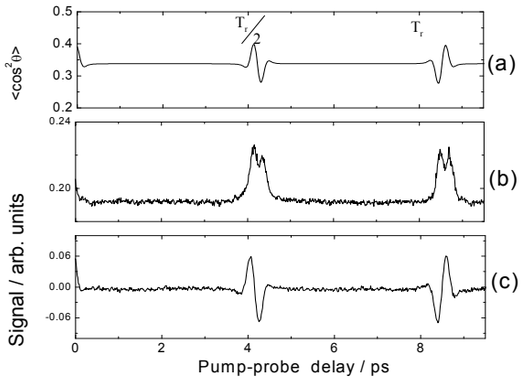

Fig. 9. Revival structure of CO irradiated by 800 nm, 110 fs at an intensity of 2×10^{13} W/cm^2 (a) Numerical calculation, (b) homodyne signal, (c) pure heterodyne signal.

Figures 7c, 8c and 9c display the pure heterodyne signal versus the pump-probe delay for N_2, O_2 and CO irradiated by 800 nm, 110 fs laser pulses at an intensity of 2×10^{13} W/cm^2. The signal was proportional to ($\langle\cos^2\theta\rangle$-1/3). Comparing with the numerical calculated alignment parameter $\langle\cos^2\theta\rangle$, there is only a baseline (~1/3) shift. Thus, the heterodyne signal directly reproduced the revival structure of molecules under the field-free condition.

2. Fourier transforms of the time-dependent alignment signals

The Fourier transform spectrum of the time-dependent alignment parameter $\langle\cos^2\theta\rangle$ signal contains a serial of beat frequencies $\Delta\omega$ between adjacent J states, which are given by:

$$\Delta\omega_{J,J+2} = \frac{E_{J+2} - E_J}{\hbar} = (4J+6)\omega_0 \tag{25}$$

where $\omega_0=2\pi B_0 c$ is the fundamental phase frequency. The amplitudes of the beat frequencies are proportional to the products of the expanding coefficients. These coefficients denoted the populations of the different |J> states in the rotational wave packet.

Figs. 10a, 11a and 12a show the Fourier transform spectra of the calculated $\langle\cos^2\theta\rangle$ in Figs. 7a, 8a and 9a. In the present study, the beat frequency $\Delta\omega$ is directly replaced by the rotational quantum number J and all the Fourier transforms of the alignment signals span three full periods of the molecules. Each spectrum describes the revival structure decomposing into different |J> states. There is a ~2:1 intensity alternation between even J and odd J states for N_2, but there are only odd J states for O_2. The difference of the relative weights between even and odd J states resulted in different alignment signals at quarter revivals for these molecules.

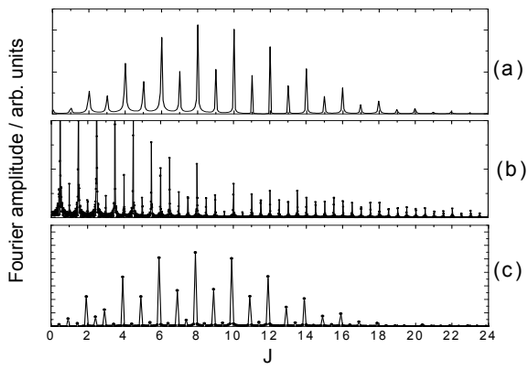

Fig. 10. Fourier transforms of the revival structure of N_2 shown in Figure 7.

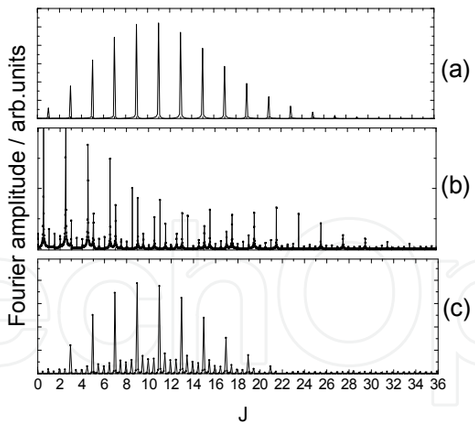

Fig. 11. Fourier transforms of the revival structure of O_2 shown in Figure 8.

Figs. 10b, 11b and 12b show the Fourier transform spectra of the homodyne signals in Figs. 7b, 8b and 9b. The beat frequencies were more than the fundamental frequencies. They also include the sum and the difference frequencies. The front progression is the difference frequencies, the middle progression is the fundamental frequencies and the end is the sum frequencies. However, the Fourier amplitudes of the fundamental frequencies were minor for the Fourier transform of the homodyne signal, even though they reflected the populations of different J states in the rotational wave packet.

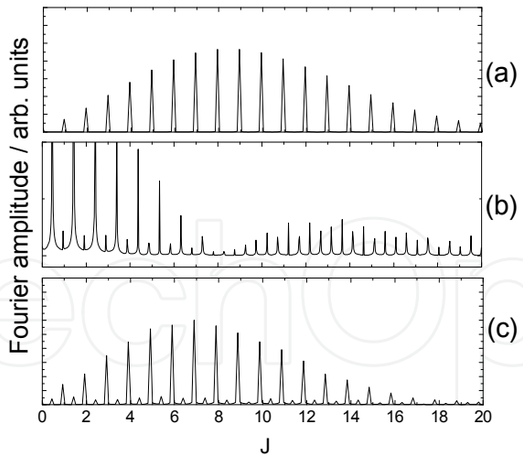

Fig. 12. Fourier transforms of the revival structure of CO shown in Figure 9.

Figs. 10c, 11c and 12c show the Fourier transform spectra of the pure heterodyne signals in Figs. 7c, 8c and 9c. In comparison with the contribution from the complicated beat frequencies in the homodyne signal, the contribution from the fundamental frequencies dominated in the Fourier transform spectrum of the pure heterodyne signal. The Fourier transform spectrum of the heterodyne signal was very similar to that of the calculated alignment parameter $\langle \cos^2 \theta \rangle$, which reflected the actual populations of different J states in the rotational wave packet.

2.3 Detection of gas component using molecular alignment

Due to the lower molecular density, field-free alignment of gas sample is more obvious than liquid and solid, which could be used in rapid detection of gas component. The experimental results bellows also demonstrated that gas mixture of N_2 and O_2 present a mixed alignment structure in which N_2 and O_2 present their own alignment structure. This result shows a feasibility of rapid detection of gas component.

Figure 13 shows the alignment signal for (a) N_2, (b) O_2, and (c) air at room temperature under one atmosphere pressure. As we know, air mainly contains N_2 and O_2. It is clearly

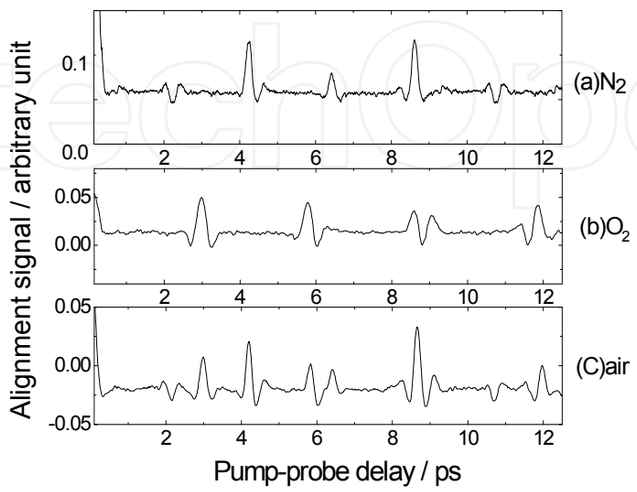

Fig. 13. Alignment signal for (a) N_2, (b) O_2, and (c) air.

seen that alignment structure of gas sample can be derived from alignment signal of pure N_2 and O_2. It is possible that one can identify the component from gas mixture rapidly if the alignment structure of pure component is obtained. Precision of this alignment detection method just depends on the value of polarization anisotropy for different molecules.This technique has two weaknesses. First, if the gas molecule is spherical, which means it has no polarization anisotropy; there will be no alignment signal. Second, if different molecules have same rotational periods, it is also hard to distinguish each molecule during the mixed alignment structure. Although this technique is not perfect, it can be used to detect different gas component easily and rapidly.

3. Conclusion

In summary, we have realized field-free alignment of N_2, O_2, CO, CO_2, CS_2, and C_2H_4 at room temperature using strong femtosecond laser pulses. We also demonstrated that the degree of alignment could be greatly improved by using two-pulse scheme with appropriate separated time. These researches indicate that multiple-pulse alignment is a feasible approach to obtain macroscopic ensembles of highly aligned molecules in the laboratory. We believe our results will promote the practical applications of field-free aligned molecules.

We modified the typical weak field polarization technique. The homodyne detection and the heterodyne detection were realized in an apparatus. They were utilized to quantify the field-free alignments of diatomic molecules N_2, O_2 and CO irradiated by strong femtosecond laser pulses. The alignment signal is proportional to $(\langle\cos^2\theta\rangle - 1/3)^2$ for homodyne detection and $(\langle\cos^2\theta\rangle - 1/3)$ for pure heterodyne detection. Fourier transform spectra of the homodyne signal and the pure heterodyne signal were also studied. Comparing with the homodyne detection, the pure heterodyne detection had the following advantages. First, the pure heterodyne signal directly reproduced the alignment parameter$\langle\cos^2\theta\rangle$ except a 1/3 baseline shift. Second, the Fourier transform spectrum of the pure heterodyne signal was very similar to that of the calculated alignment parameter $\langle\cos^2\theta\rangle$ and reflected the actual populations of different *J* states in the rotational wave packet.

Different gas samples present different alignment structure. We also demonstrated that N_2 and O_2 component can be identified by measuring alignment structure of an air sample. This result will promote the applications of femtosecond laser in gas component detection and other fields.

4. References

T. Seideman, *Time-resolved photoelectron angular distributions as a means of studying polyatomic nonadiabatic dynamics*, J. Chem. Phys., 2000. 113: p. 1677 .

T. Seideman, *Time-resolved photoelectron angular distributions as a probe of coupled polyatomic dynamics*, Phys. Rev. A, 2001. 64: p. 042504.

T. P. Rakitzis, A. J. van den Brom, and M. H. M. Janssen, *Directional dynamics in. photodissociation of oriented molecules*, Science, 2004. 303: p. 852.

V. Aquilanti, M. Bartolomei, F. Pirani, D. Cappelletti, Vecchiocattivi, Y. Shimizu, and T. Kasai, *Orienting and aligning molecules for stereochemistry and photodynamics*, Phys. Chem. Chem. Phys., 2005.7: p. 291.

N. Mankoc-Borstnik, L. Fonda, and B. Borstnik, *Coherent rotational states and their creation and time evolution in molecular and nuclear systems*, Phys. Rev. A, 1987. 35: p. 4132.

R. A. Bartels, T. C. Weinacht, N. Wagner, M. Baertschy, C. H. Greene, M. M. Murnane, and H. C. Kapteyn, *Phase Modulation of Ultrashort Light Pulses using Molecular Rotational Wave Packets*, Phys. Rev. Lett., 2002. 88: p. 013903.

S. Ramakrishna and T. Seideman, *Intense Laser Alignment in Dissipative Media as a Route to Solvent Dynamics*, Phys. Rev. Lett., 2005. 95: p. 113001.

K. F. Lee, D. M. Villeneuve, P. B. Corkum, and E. A. Shapiro, *Phase Control of Rotational Wave Packets and Quantum Information*, Phys. Rev. Lett., 2004. 93: p. 233601.

J. Itatani, J. Levesque, D. Zeidler, H. Niikura, H. Pepin, J. C. Kieffer, P. B. Corkum, and D. M. Villeneuve, *Tomographic imaging of molecular orbitals,* Nature (London) 2004. 432: p. 867.

J. G. Underwood, B. J. Sussman, A. Stolow, *Field-Free Three Dimensional Molecular Axis Alignment*, Phys. Rev. Lett., 2005. 94: p. 143002.

Hertz E, Daems D, Guerin S, et al., Field-free molecular alignment induced by elliptically polarized laser pulses: Noninvasive three-dimensional characterization, Phys. Rev. A, 2007. 76: p. 043423.

Lee KF, Villeneuve DM, Corkum PB, et al. *Field-free three-dimensional alignment of polyatomic molecules*, Phys. Rev. Lett., 2006. 97: p. 173001.

R. de Nalda, C. Horn, M. Wollenhaupt, M. Krug, L. Banares and T. Baumert, *Pulse shaping control of alignment dynamics in* N_2, J. Raman Spectrosc., 2006. 38 (5): p. 543.

Christer Z. Bisgaard, Mikael D. Poulsen, Emmanuel Pe´ronne, Simon S. Viftrup, and Henrik Stapelfeldt, *Observation of Enhanced Field-Free Molecular Alignment by Two Laser Pulses*, Phys. Rev. Lett., 2004. 92: p. 173004.

P.W. Dooley, I.V. Litvinyuk, K.F. Lee, D.M. Rayner, M. Spanner, D.M. Villeneuve, P.B. Corkum, *Direct imaging of rotational wave-packet dynamics of diatomic molecules*, Phys. Rev. A, 2003. 68: p. 023406.

V. Renard, M. Renard, S. Guerin, Y.T Pashayan, B. Lavorel, O. Faucher, H.R. Jauslin, *Postpulse Molecular Alignment Measured by a Weak Field Polarization Technique*, Phys. Rev. Lett., 2003. 90: p. 153601.

A. Rouzee, V. Renard, B. Lavorel, O. Faucher, *Laser spatial profile effects in measurements of impulsive molecular alignment*, J. Phys. B, 2005. 38 : p. 2329.

V. Renard, O.Faucher, B. Lavorel, *Measurement of laser-induced alignment of molecules by cross defocusing*, Opt. Lett., 2005. 30: p. 70.

S.Zamith, Z. Ansari, F. Lepine, M.J.J. Vrakking, *Measurement of laser-induced alignment of molecules by cross defocusing*, Opt. Lett., 2005. 30: p. 2326.

R.W. Boyd. *Nonlinear Optics*. Academic Press, California USA, 1992.

W.H. Press et al., *Numerical Recipes*, 2nd ed. Cambridge University Press, Cambridge, England, 1992.

C.Z. Bisgaard, M.D. Poulsen, E. Peronne, S.S. Viftrup, H. Stapelfeldt, *Observation of Enhanced Field-Free Molecular Alignment by Two Laser Pulses*, Phys. Rev. Lett., 2004. 92: p. 173004.

G. Herzberg, *Molecular spectra and molecular structure*, Van Nostrand Reinhold Company Ltd., 1966.

S.Ramakrishna,T. Seideman, *Dissipative dynamics of laser induced nonadiabatic molecular alignment*, J. Chem. Phys., 2006. 124: p. 034101.

Rouzée, A.; Guérin, S.; Boudon, V.; Lavorel, B.; Faucher, O. *Field-Free One-Dimensional Alignment of Ethylene Molecule*. Phys. Rev. A 2006, 73, 033418.

P.B. Corkum, C. Ellert, M. Mehendale, P. Dietrich, S. Hankin, S. Aseyev, D. Rayner, D. Villeneuve, Faraday Discuss., 113, 47 (1999)

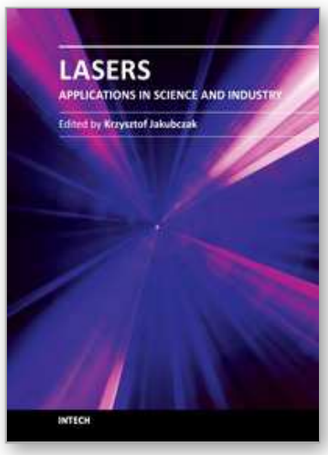

Lasers - Applications in Science and Industry
Edited by Dr Krzysztof Jakubczak

ISBN 978-953-307-755-0
Hard cover, 276 pages
Publisher InTech
Published online 09, December, 2011
Published in print edition December, 2011

The book starts with basic overview of physical phenomena on laser-matter interaction. Then it is followed by presentation of a number of laser applications in the nano-particles and thin films production, materials examination for industry, biological applications (in-vitro fertilization,tissue ablation) and long-range detection issues by LIDARs.

How to reference
In order to correctly reference this scholarly work, feel free to copy and paste the following:

Nan Xu, Jianwei Li, Jian Li, Zhixin Zhang and Qiming Fan (2011). Polarization Detection of Molecular Alignment Using Femtosecond Laser Pulse, Lasers - Applications in Science and Industry, Dr Krzysztof Jakubczak (Ed.), ISBN: 978-953-307-755-0, InTech, Available from: http://www.intechopen.com/books/lasers-applications-in-science-and-industry/polarization-detection-of-molecular-alignment-using-femtosecond-laser-pulse

INTECH
open science | open minds

InTech Europe
University Campus STeP Ri
Slavka Krautzeka 83/A
51000 Rijeka, Croatia
Phone: +385 (51) 770 447
Fax: +385 (51) 686 166
www.intechopen.com

InTech China
Unit 405, Office Block, Hotel Equatorial Shanghai
No.65, Yan An Road (West), Shanghai, 200040, China
中国上海市延安西路65号上海国际贵都大饭店办公楼405单元
Phone: +86-21-62489820
Fax: +86-21-62489821

IntechOpen